*Desalination and Water Treatment*
www.deswater.com
doi: 10.1080/19443994.2016.1164083

57 (2016) 26440–26447
November

Taylor & Francis
Taylor & Francis Group

# Functionalized PolyHIPE polymer monoliths as an anion-exchange media for removal of nitrate ions from aqueous solutions

Necla Barlık[a,*,1], Bülent Keskinler[b], M. Muhtar Kocakerim[c], Galip Akay[d,e]

[a]*Engineering Faculty, Department of Environmental Engineering, Atatürk University, Erzurum 25240, Turkey, Tel. +90 478 211 7531; Fax: +90 478 211 7532; email: neclabarlik@ardahan.edu.tr*
[b]*Department of Environmental Engineering, Gebze Technical University, Gebze Kocaeli 41400, Turkey, email: bkeskinler@gyte.edu.tr*
[c]*Engineering Faculty, Department of Chemical Engineering, Çankırı Karatekin University, Çankırı 18000, Turkey, email: mkocakerim@karatekin.edu.tr*
[d]*School of Chemical Engineering and Advanced Materials, Newcastle University, Newcastle upon Tyne NE1 7RU, UK, emails: galip.akay1@gmail.com, galipakay@basari.edu.tr*
[e]*GAP Technologies Ltd., 1 Grosvenor Place, 8th Floor, London SW1X 7HJ, UK*

Received 26 November 2015; Accepted 6 March 2016

---

## ABSTRACT

Monolithic anion exchanger PolyHIPE media were used for the removal of nitrate anions ($NO_3^-$) from aqueous solutions. Both equilibrium and column $NO_3^-$ adsorption tests and regeneration tests were carried out. The suitability of the Langmuir adsorption model to the equilibrium data was investigated. The maximum adsorption capacity was 0.215 meq/g as per Langmuir isotherm at 20˚C. At a flow rate of 5 ml/min (corresponding flux was 1.0 cm/min) and 150 mg/L nitrate feed concentration, breakthrough capacity and apparent capacity were 1.336 meq $NO_3^-$/g resin and 2.842 meq $NO_3^-$/g resin, respectively. Column experimental tests were conducted to provide data for theoretical modeling and to verify the system performance of the process. The theoretical column model adopted in this work was found to describe well, the ion-exchange breakthrough characteristics. After reaching equilibrium adsorption capacity, the monoliths were regenerated using 1 N HCl and were subsequently retested. It was found that the regeneration efficiency reduced from 99% after second usage to 95% after the third usage.

*Keywords:* Monolithic anion exchanger; Nitrate removal; Mathematical modeling; Regeneration efficiency

---

## 1. Introduction

Highly porous microcellular foams, known as PolyHIPE Polymers (PHPs) were synthesized through high internal phase emulsion (HIPE) polymerization. These materials having a fully interconnected morphology are cross-linked styrene–divinylbenzene copolymer formations [1–8]. The applications of PolyHIPEs are now extensive; they are used either as monolithic micro-reactors for chemical or biochemical

---

*Corresponding author.

[1] Present address: Engineering Faculty, Department of Environmental Engineering, Ardahan University, 75000 Ardahan, Turkey.

conversions, or absorbents or membranes, or indeed as a combination of these three basic modes of operation. In most small- or large-scale applications of PolyHIPEs, such as in agriculture [9–11], biotechnology/medicine [12–14], separation [15,16], and environmental processes [17–20], the bulk or surface functionality of PolyHIPE requires ion-exchange capacity. The required anionic or cationic characteristics are dictated by the nature of the application. Anionic materials generally contain functional groups such as carboxyl and sulfone. Functional groups such as quaternary ammonium groups are present in cationic materials. Cation exchanger PolyHIPEs were produced via the surface modification of the PolyHIPE-based styrene and di vinylbenzene copolymer. These PolyHIPEs have been used in agricultural and separation processes [9–11,15,16,18].

Underground drinking waters contain many minerals in a dissolved state. Waste water, both from domestic and industrial/agricultural sources, are essentially polluted with ionic and molecular species which must be removed before water recycling. Nitrate is one such pollutant which when in excess may cause various infectious diseases such as methemoglobinaemia in newborn children. The actual toxin is in fact nitrite that is formed by the reduction of nitrate by intestinal bacteria. Nitrite reacts with amines in an acidic medium to form nitrosamines which are carcinogens and mutagens [21].

Nitrate pollution in surface and underground waters arises from two sources, decomposition of organic matter and fertilizer usage. Part of the nitrate in soil is taken up by plants and the rest mixes into surface and underground waters and pollutes them. Maximum permitted nitrate level for drinking water is 25 mg/L according to EU standards [22]. WHO and US EPA have set a maximum contaminant level of 50 mg/L [23] and 10 mg/L [24] of $NO_3^-$ in drinking water, respectively.

Various methods based on chemical, physical, or biological processes have been applied for removing nitrate in water. Traditional methods are chemical processes such as reverse osmosis [25], catalytic reduction [26,27], ion exchange [28,29] and biological processes such as denitrification [30,31]. Among these applications, the ion-exchange processes (using functionalized membranes or anion-exchange resins) are suitable for the removal of nitrate pollutants because of their high selectivity, simplicity, effectiveness, and relatively low cost [32–37]. The goal of this research is to determine the removing capability of nitrate ions of the anion exchanger PolyHIPE monoliths [38] prepared in our laboratory. For this purpose, equilibrium and column ion adsorption tests were performed by these monoliths (disk shaped) in nitrate removal from potassium nitrate solutions. Also, these ion adsorption data were compared with mathematical models. Tests were also carried out after the monoliths were regenerated using hydrochloric acid.

## 2. Materials and methods

### 2.1. Materials

The anion exchanger disks were prepared in our laboratory [38] based on the fundamental study reported by Akay [39,40]. They were produced by the bonding pyridine group to chloromethylated crosslinked PolyHIPE. $KNO_3$ and HCl (used for respectively the preparation of aqueous nitrate solution as the model polluted water and for the regeneration of the PolyHIPE disks) were reagent—grade Merck products.

### 2.2. Methods

In the ion adsorption tests, PolyHIPE anion exchanger disks with 2.54 cm in diameter and 0.3 cm in thickness were used as a bed of exchange media. In the preparation of the stock solution of nitrate, deionized water and reagent grade $KNO_3$ were used. The nitrate adsorption and column tests were carried out at room temperature and at pH 5.30 ± 0.05. An apparatus made entirely from plastic components was used to house the disk of known dry mass. The modules were closed at one end so the solution passed radially through into a central drainage channel. The concentration of nitrate ions was determined with an UV–160 Shimadzu spectrophotometer by measuring the absorbance at 220 nm.

#### 2.2.1. Equilibrium ion adsorption tests

The feed solution was circulated between the disk and a stirred container via a peristaltic pump (stable flow rate of 10 ml/min). The apparatus is shown schematically in Fig. 1.

Initially, the concentration of 50 mg/L, and the volume of 250 ml were set in flask. The concentration of $NO_3^-$ in the circulating solution was allowed to reach equilibrium which was determined by periodic sampling of the solution in the flask. After the steady state was reached (the concentration in the flask was permanent over time), the solution concentration was increased by adding small amount of concentrated nitrate solution. The circulation has been continued until it reaches the steady state again.

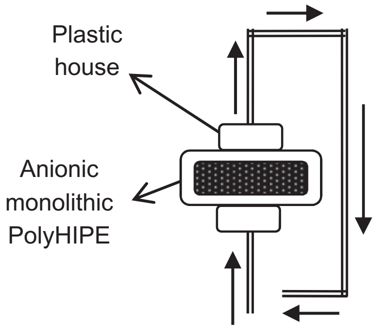

Fig. 1. A schematic diagram of the apparatus used for equilibrium ion adsorption.

### 2.2.2. Column ion adsorption tests

Single-pass tests were conducted using the apparatus shown in Fig. 1. A constant flow rate (5 ml/min) of feed solution was maintained through the anion exchanger PolyHIPE disk. The tests were performed in an up-flow mode. The apparatus was also used in the column tests. But the feed solution was drained above the plastic house, not circulated. Feed concentrations of 15, 30, 75, and 140 mg $NO_3^-$/L, and flows rates of 5, 10, and 20 ml/min were chosen thus providing a flux rate range of 1–4 cm/min. The concentration of the effluent was monitored with time, until it was the same as the feed concentration.

### 2.2.3. Regeneration of anion exchanger monoliths

1 N HCl was used as the regenerant and experiments were performed in column adsorption tests' apparatus as Fig. 1. The operation was referred to as countercurrent ion exchange. Service was in up-flow and regeneration was in down-flow mode. Feed concentration of 100 mg $NO_3^-$/L, and flows rates of 10 ml/min were chosen in services. Regenerant solution flowed down 0.5 ml/min. After service or regeneration, anion exchanger media was washed with excess distilled water. Service and regeneration were performed three times and two times, respectively.

## 3. Results and discussion

### 3.1. Equilibrium ion adsorption tests

The chemical structure of the PolyHIPE with anionic functionality can be represented as [38] (Fig. 2).

Equilibrium between the anion exchanger media and nitrate ions can be represented by the following equilibrium reaction:

$$R-CH_2N^+\,Cl^- + NO_3^- \rightleftarrows R-CH_2N^+NO_3^- + Cl^- \tag{1}$$

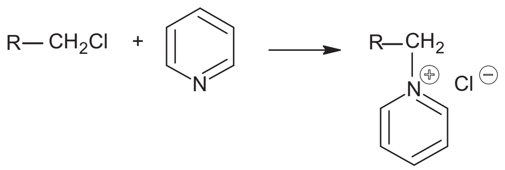

Fig. 2. The chemical structure of anionic PolyHIPE Polymer.

where R–$CH_2$ $N^+$ $Cl^-$ represents the repeating structure of PolyHIPE. In the evaluation of the anionic PolyHIPE, the mass of nitrate on the anion exchanger was calculated and isotherm showing the amount of nitrate per gram of anion exchanger against the equilibrium concentration in the solution was plotted. The anion exchanger disks produced isotherm that was similar in shape to that of a Type I adsorption isotherm, which can be described by the Langmuir equation [41]. The Langmuir isotherm model is a well-known and widely used model in the literature [17,28]. The model assumes monolayer adsorption onto surfaces that take place at the finite number of identical sites [42,43]. There are no lateral interactions between neighboring adsorbed molecules. The Langmuir relation is stated as Eq. (2):

$$q_e = \frac{q_{max} K_L c_e}{1 + K_L c_e} \tag{2}$$

In Eq. (3), $c_e$ is the equilibrium nitrate ions concentration in solution (mg/L), $q_e$ is the amount of nitrate ions adsorbed at equilibrium (mg $g^{-1}$), $q_{max}$ is the monolayer capacity of the adsorbent (mg $g^{-1}$), and $K_L$ is the Langmuir constant and related to the energy of adsorption. In order to calculate $q_{max}$ and $K_L$ parameters, Eq. (2) can be rearranged to give the following linear equation:

$$\frac{c_e}{q_e} = \frac{K_L}{q_{max}} + \frac{c_e}{q_{max}} \tag{3}$$

The plots of $c_e/q_e$ vs. $c_e$ for the adsorption of nitrate ions onto the monolithic anionic PolyHIPE (Fig. 3) give a straight line of slope $1/q_{max}$ and intercept $K_L/q_{max}$. The Langmuir coefficient and maximum adsorption capacity for the anion exchanger PolyHIPE disks were obtained as 51.806 L/g and 0.215 meq $NO_3^-$/g resin, respectively with $R^2$ of 0.994.

### 3.2. Column ion adsorption tests

Ion exchange is a process whose performance is affected by a number of operational parameters,

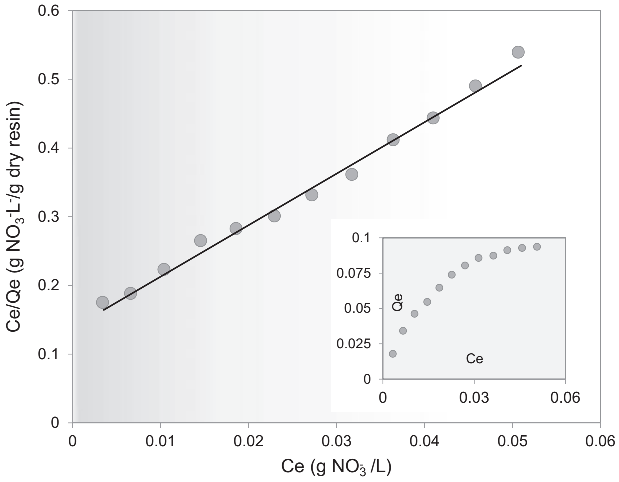

Fig. 3. Langmuir plots for the adsorption of $NO_3^-$ by anion exchanger PolyHIPE monoliths.

including the equilibrium resin adsorption capacity and the mass transfer rate. The capacity of an anion exchanger can be expressed in a number of ways. Titrimetric analysis can be used to determine the ion-exchange capacity, i.e. the number of ionic groups for a given amount of resin; when in the $Cl^-$ form this can be interpreted as the "total," "scientific weight" capacity. Under some operating conditions not all the available counter ions may take part in the exchange process, giving rise to the capacity under specific operating conditions; this is the so-called "apparent" (or effective) capacity. In this process, the reaction between resin and nitrate ions can be represented by the reaction as in Eq. (1).

A value for the breakthrough capacity and the apparent capacity of the disks (for $NO_3^-$) can be estimated from the effluent profiles by calculating the area between the adsorption curve and a line representing the concentration of the outlet solution. The area under the breakthrough curve represents the mass of challenge ions adsorbed onto 1 g of resin material. Breakthrough occurs when the concentration of the effluent stream rises above zero. The capacity which is utilized until breakthrough occurs is called the "breakthrough" (or dynamic) capacity.

Table 1 is listed the breakthrough and the apparent capacities and volumes of the disks depending the operation conditions.

Sherman [44] obtained the following equation for the accumulation of solute on porous solid adsorbent:

$$(D_\mathrm{M} + D_\mathrm{L})\frac{\partial^2 c}{\partial z^2} - \frac{q}{A\varepsilon}\frac{\partial c}{\partial z} = \left(1 + \frac{(1-\varepsilon)}{\varepsilon}K\right)\frac{\partial c}{\partial t} \tag{4}$$

where $D_\mathrm{M}$ is the molecular dispersion coefficient ($m^2/s$), $D_\mathrm{L}$ is the longitudinal dispersion coefficient ($m^2/s$), $c$ is the concentration of effluent from bed (mg/L), $\varepsilon$ is porosity of the bed, $K$ is an equilibrium constant for adsorption, $z$ is the distance variable in the direction of flow (m), $t$ is time (s), $q$ is flow rate ($m^3/s$), and $A$ is the cross sectional area of the bed ($m^2$). $D_\mathrm{M}$ is small compared to $D_\mathrm{L}$ for very low flow rates. Therefore, Eq. (4) could be rearranged as follows:

$$D_\mathrm{L}\frac{\partial^2 c}{\partial z^2} - \frac{q}{A\varepsilon}\frac{\partial c}{\partial z} = \frac{1}{\lambda}\frac{\partial c}{\partial t} \tag{5}$$

$$\frac{c}{c_0} = 1 - \frac{1}{2}\left[\operatorname{erfc}\left(\frac{1-R\lambda}{2\sqrt{R\lambda S}}\right) + \exp\left(\frac{1}{S}\right)\operatorname{erfc}\left(\frac{1+R\lambda}{2\sqrt{R\lambda S}}\right)\right] \tag{6}$$

where $\lambda = \varepsilon/\varepsilon + K(1-\varepsilon)$, $R = qt/A\varepsilon z$ and $S = A\varepsilon D_\mathrm{L}/qz$.

The least square was used to estimate the constants $D_\mathrm{L}$ and $K$ by minimizing the error function $F$ defined as:

$$F = \sum_{i=1}^{np}\left[(c/c_0)_{\mathrm{EXPT.}} - (c/c_0)_{\mathrm{MODEL}}\right]^2 \tag{7}$$

Table 1
Capacity of anion exchanger PolyHIPE disks to remove $NO_3^-$

| Flow rate (ml/min) | Feed concentration (mg/L) | Breakthrough capacity (meq $NO_3^-$/g anion exc. PHP) | Apparent capacity (meq $NO_3^-$/g anion exc. PHP) | Breakthrough volume (L/g anion exc. PHP) | Apparent volume (L/g anion exc. PHP) |
|---|---|---|---|---|---|
| 5 | 15 | 1.660 | 2.377 | 7.89 | 17.34 |
| 10 | 15 | 1.491 | 1.885 | 6.86 | 13.04 |
| 20 | 15 | 1.417 | 1.708 | 6.35 | 12.01 |
| 5 | 30 | 1.432 | 2.271 | 3.01 | 10.66 |
| 5 | 75 | 1.446 | 2.064 | 1.24 | 3.69 |
| 5 | 140 | 1.070 | 1.893 | 0.43 | 2.26 |

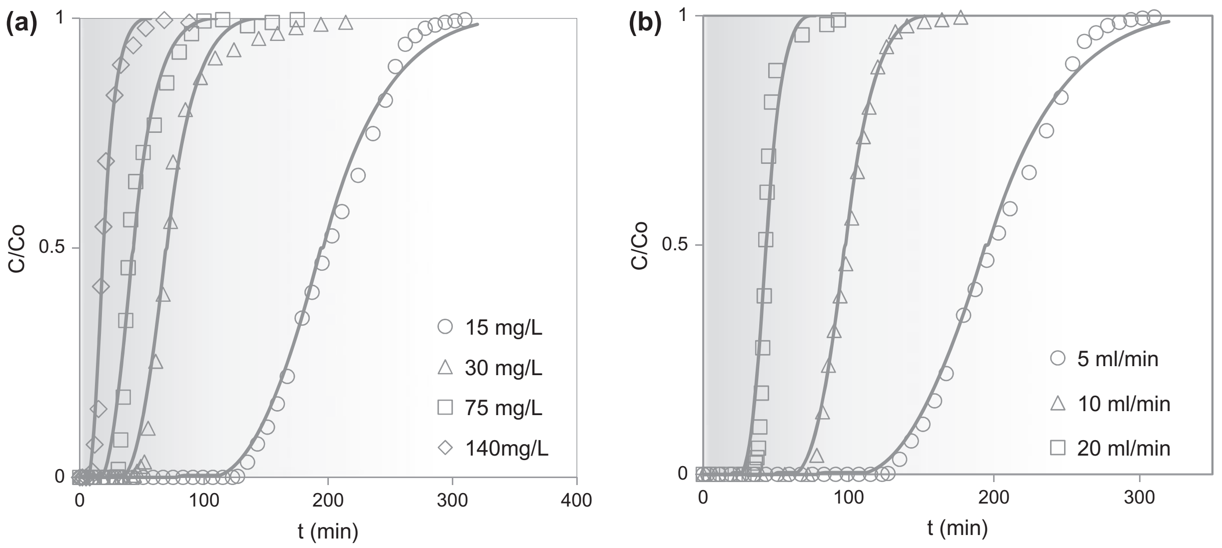

Fig. 4. Comparison of $(c/c_0)_{\mathrm{MODEL}}$ (lines) and $(c/c_0)_{\mathrm{EXPT.}}$ (dots) $NO_3^-$ adsorption breakthrough curves of the anion exchanger PolyHIPE monoliths for different feed concentrations (5 ml/min of flow rate, at pH 5.30 ± 0.05 and room temperature) (a) and, for different flow rates (15 mg/L of feed concentrations, at pH 5.30 ± 0.05 and room temperature) (b).

Table 2
The adsorption equilibrium constant (*K*) and the dispersion coefficient ($D_L$) determined from the mathematical model in which the error function (*F*) is minimized

| Flow rate (ml/min) | Feed concentration (mg/L) | *K* | $D_L \times 10^{-7}$ (m$^2$/s) |
|---|---|---|---|
| 5 | 15 | 7,581 | 0.361 |
| 10 | 15 | 7,588 | 0.400 |
| 20 | 15 | 6,735 | 1.100 |
| 5 | 30 | 2,740 | 0.503 |
| 5 | 75 | 1,92 | 1.066 |
| 5 | 140 | 860 | 1.430 |

A MATLAB code was developed to estimate values of $D_{\mathrm{L}}$ and *K* and to calculate theortical effective concentration ($(c/c_0)_{\mathrm{MODEL}}$), then experimental effective concentration ($(c/c_0)_{\mathrm{EXPT.}}$) and $(c/c_0)_{\mathrm{MODEL}}$ profiles are plotted as Fig. 4(a) and (b). The values of $D_{\mathrm{L}}$ and *K* are listed in Table 2.

The effect of feed nitrate concentration on ion adsorption capacity was investigated (Fig. 4(a)). The breakthrough time and the treated volume of water decreased with the rise in feed concentration (Table 1). This indicates that the monolith bed was saturated faster by nitrate at higher concentrations due to higher nitrate loading rates. As reported in Table 1, the apparent capacity and breakthrough of these experiments are all between 1.893 to 2.377 meq $NO_3^-$/g anion exc. PHP and 1.070 to 1.660 meq $NO_3^-$/g anion exc. PHP, respectively.

The breakthrough curves of column tests of different flow rates can be found in Fig. 4(b). This figure shows that the breakthrough time generally occurred faster with higher flow rates. The breakthrough capacity

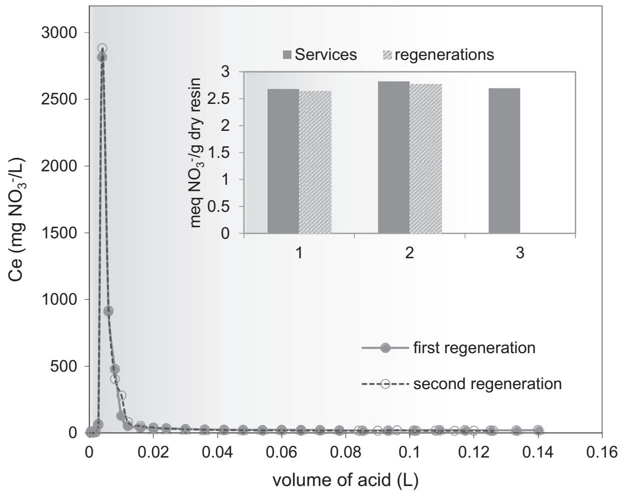

Fig. 5. Regeneration performances of the anion exchanger monoliths with 1 N HCl after services.

Table 3
Regeneration efficiency

| | Regenerant volume (L) | Regeneration efficiency $\frac{(\text{meq NO}_3^-)_{\text{removed}}}{(\text{meq NO}_3^-)_{\text{recovery}}}$ |
|---|---|---|
| First regeneration | 0.123 | 0.987 |
| Second regeneration | 0.124 | 0.949 |

changes from 1.660 to 1.417 meq $NO_3^-$/g anion exc. PHP when the flow rate changes from 5 to 20 ml/min. The apparent capacity of these experiments is from 2.377 to 1.885 meq $NO_3^-$/g anion exc. PHP. It seems that the nitrate adsorption capacity is impressed by flow rate. The plotted Fig. 4(a) and (b) in this research is comparable to those reported by other researcher [34] for both flow rates and feed concentrations.

The experimental data ($(c/c_0)_{\text{MODEL}}$) and the model prediction ($(c/c_0)_{\text{EXPT.}}$) are also provided in Fig. 4(a) and (b). There was a close agreement between the simulated and experimental breakthrough curves in several column experiments, including those with different flow rates and feed nitrate concentrations. The dispersion ($D_L$) and adsorption ($K$) coefficients were estimated for each column experiment, the results appear in Table 2.

Table 2 shows that the estimated values of $D_L$ for different feed concentrations are between $0.361 \times 10^{-7}$ and $1.430 \times 10^{-7}$ $m^2/s$. Therefore, the dispersion coefficient is influenced by feed nitrate concentration. An increase in the value of $D_L$ was observed alongside a rise in the flow rate.

### 3.3. Regeneration

The regeneration reaction is the reciprocal of adsorption reaction as given in Eq. (1). Fig. 5 shows typical regeneration profiles for ion exchanger resins in which 120 ml 1 N HCl for each regeneration. The column chart shows service performances and regeneration performances for the anion exchanger monoliths, sequentially. The services have been repeated three times for 100 mg/L of feed concentration and 10 ml/min of flow rate. The regeneration performances have been repeated two times. Also, the capacity of the monolith does not show a significant decrease after the third service.

Regeneration efficiency is defined as the ratio of the total equivalents of ions removed from a resin to the total equivalents of ions present in the volume of regenerant used [45]. The regeneration efficiency determined for anion exchanger disks with 1 N HCl is listed in Table 3.

## 4. Conclusions

The ion-exchange behavior of the resins depends chiefly on the nature of the fixed ionic groups. Important factors are the acid or base strength of the groups and specific interactions with the counter ions. Counter ions which associate with the fixed ionic groups are preferred by the resin [43].

The anion-exchange monoliths were examined to remove the nitrate ions from the aqueous solutions with various nitrate ion concentrations and flow rates. The results showed that the nitrate adsorption capacity was increased with increasing the contact time and decreased with increasing the initial nitrate concentration. Model parameters gave a very good fitting of experimental data $NO_3^-$ removal with anion exchangers disks. The column adsorption data were well fitted by the mathematical model. In addition, the equilibrium isotherm values were well fitted to the Langmuir isotherm model.

The experimental results indicated that anion exchanger PolyHIPE disk media acted as an anion exchanger resin to remove nitrate ions from aqueous solution. $KNO_3$ solution was used in ion-exchange experiments. Potassium has a relatively large (1.38 Å) ionic radius, so it can be expected that the exchange process and the adsorption capacity have been influenced negatively.

In time, an electrical charge balance is formed at between the nitrate ions in the solution and the chlorine ions on the anion-exchange medium, then the ion exchange almost ends for the equilibrium tests. For the column tests, it is fed the stock nitrate solution to the process, continuously. The equilibrium of the reaction (Eq. (1)) progresses on the right. Therefore, the breakthrough capacity is greater than $q_{\max}$, derived from the result of the equilibrium tests.

Anion exchanger media can be regenerated using 1 N HCl. Ideally, regeneration should not cause any loss of the total exchange capacity. In the present study, it was found that the first regeneration efficiency was determined as 98.7%, while the second regeneration efficiency was 94.9%. Therefore, the regenerated disk can be effectively used for $NO_3^-$ adsorption although we only regenerated the monoliths only twice.

The anion exchanger PolyHIPE used as a monolith is attractive as a potential adsorbent for the anion removal from aqueous solutions as its response is fast because of the accessibility of the exchange sites through the hierarchic pore structure.

## Acknowledgment

Research Fund of Ataturk University, Turkey sponsored the PhD studentship of Dr Necla Barlık. Further support was received for Prof Galip Akay from the European Union under the integrated project, POLYCAT (Contract No: CP-IP 246095-2 POLYCAT) when he led the project at Newcastle University.

## List of symbols

$c_e$ — equilibrium nitrate ions concentration in solution, mg/L
$q_e$ — amount of nitrate ions adsorbed at equilibrium, mg $g^{-1}$
$q_{max}$ — monolayer capacity of the adsorbent, mg $g^{-1}$
$K_L$ — Langmuir constant and related to the energy of adsorption, L $mg^{-1}$
$D_M$ — molecular dispersion coefficient, $m^2$ $s^{-1}$
$D_L$ — longitudinal dispersion coefficient, $m^2$ $s^{-1}$
$c$ — concentration of effluent from bed, mg/L
$c/c_0$ — effective concentration
$\varepsilon$ — porosity of the bed
$K$ — equilibrium constant for adsorption
$z$ — distance variable in the direction of flow, m
$t$ — time, s
$q$ — flow rate, $m^3$ $s^{-1}$
$A$ — cross sectional area of the bed, $m^2$

## References

[1] Z. Haq, Porous cross-linked absorbent polymeric materials, US Patent: 4536521, 1985.

[2] A.Y. Sergienko, H. Tai, M. Narkis, M.S. Silverstein, Polymerized high internal-phase emulsions: Properties and interaction with water, J. Appl. Polym. Sci. 84 (2002) 2018–2027.

[3] G. Akay, A. Bokhari, V. Byron, M. Dogru, Development of Nano Structured Materials and Their Application in Bioprocess, Chemical Process Intensification and Tissue Engineering, Chemical Engineering Trends and Developments, Wiley, London, 2005.

[4] A. Desforges, M. Arpontet, H. Deleuse, O. Mondain-Monval, Synthesis and functionalization of polyHIPE® beads, React. Funct. Polym. 53 (2002) 183–192.

[5] N.R. Cameron, High internal phase emulsion templating as a route to well-defined porous polymers, Polymer 46 (2005) 1439–1449.

[6] G. Akay, Z.Z. Noor, O. Calkan, T. Ndlovu, D.R. Burke, Microwave Functionalisation of PolyHIPE, US Patent: 7820729, 2010.

[7] G. Akay, B. Calkan, H. Hasan, R. Mohamed, Preparation of nano-structured microporous composite foams, European Patent: 2342272, 2013.

[8] G. Akay, S. Dawnes, V.J. Price, Microcellular polymers as cell growth media and novel polymers, European Patent: 1183328, 2012.

[9] G. Akay, D. Burke, AgroProcess intensification through synthetic rhizosphere media for nitrogen fixation and yield enhancement, Am. J. Agric. Biol. Sci. 7 (2012) 150–172.

[10] G. Akay, S. Fleming, AgroProcess intensification: Micro-bioreactors as soil additives with nitrogen fixing bacterium azospirillum brasilense to enhance its potential as self-sustaining biofertiliser, Green Process. Synth. 1 (2012) 227–237.

[11] G. Akay, D. Burke, Synthetic symbiotic system as soil additives to deliver active ingredients through plant roots for enhanced plant and crop yield, US Patent, European Patent: 8898955, 2349362, 2014.

[12] G. Akay, M. Birch, M. Bokhari, Microcellular polyHIPE polymer supports osteoblast growth and bone formation *in vitro*, Biomaterials 25 (2004) 3991–4000.

[13] M. Bokhari, G. Akay, S. Zhang, M. Birch, The enhancement of osteoblast growth and differentiation *in vitro* on a peptide hydrogel—PolyHIPE polymer hybrid material, Biomaterials 26(25) (2005) 5198–5208.

[14] G. Akay, E. Erhan, B. Keskinler, Bioprocess intensification in flow-through monolithic microbioreactors with immobilized bacteria, Biotechnol. Bioeng. 90 (2005) 180–190.

[15] G. Akay, J. Vickers, Methods for separating oil and water, US Patent, European Patent: 7780854, 1307402, 2012.

[16] G. Akay, T. Pekdemir, A.M. Shakorfow, J. Vicker, Intensified demulsification and separation of thermal oxide reprocessing interfacial crud (THORP-IFC) simulants, Green Process. Synth. 1 (2012) 109–127.

[17] R.J. Wakeman, Z.G. Bhumgara, G. Akay, Ion exchange modules formed from polyhipe foam precursors, Chem. Eng. J. 70 (1998) 133–141.

[18] N. Barlik, B. Keskinler, Sulfonation of crosslinked styrene/divinyl benzene copolymers beads formed from porous foam and ion adsorption of copper by them: Column adsorption modeling, Water Sci. Technol. 69 (2014) 286–292.

[19] N. Barlık, Using Potential of PHP Foams in Water and Wastewater Purification Processes (Turkish), Atatürk University, Graduate School of Natural and Applied Science, Erzurum, 2006.

[20] M. Dogru, G. Akay, Gasification, Japanese Patent; US Patent: 2006-53894; 08486168, 2011; 2013.

[21] N. Lohumi, S. Gosain, A. Jain, V.K. Gupta, K.K. Verma, Determination of nitrate in environmental water samples by conversion into nitrophenols and solid phase extraction−spectrophotometry, liquid chromatography or gas chromatography–mass spectrometry, Anal. Chim. Acta 505 (2004) 231–237.

[22] M. Radojevic, V. Bashkin, Practical Environmental Analysis, Royal Society of Chemistry, Cambridge, 1999.

[23] S.B. Hamouda, K. Touati, M.B. Amor, Donnan dialysis as membrane process for nitrate removal from drinking water: Membrane structure effect, Arabian J. Chem. (2012) (available online).

[24] US Environmental Protection Agency, Drinking Water Standards and Health Advisories, US Environmental Protection Agency, Office of Water, Washington, DC, 2012.
[25] J. Schoeman, A. Steyn, Nitrate removal with reverse osmosis in a rural area in South Africa, Desalination 155 (2003) 15–26.
[26] J. Reddy, J. Lin, Nitrate removal from ground water using catalytic reduction, Water Res. 34 (2000) 995–1001.
[27] A. Pintar, J. Batista, J. Levec, Integrated ion-exchange/catalytic process for efficient removal of nitrates from drinking water, Chem. Eng. Sci. 56 (2001) 1551–1559.
[28] M. Chabani, A. Amrane, A. Bensmaili, Kinetic modelling of the adsorption of nitrates by ion exchange resin, Chem. Eng. J. 125 (2006) 111–117.
[29] S.H. Lin, C.L. Wu, Nitrite and nitrate removal from aqueous solution by Ion exchange, J. Environ. Sci. Health Part A: Environ. Sci. Eng. Toxicol. 32(5) (1997) 1575–1589.
[30] M. Boumediene, D. Achour, Denitrification of the underground waters by specific resin exchange of ion, Desalination 168 (2004) 187–194.
[31] K. Kimura, M. Nakamura, Y. Watanabe, Nitrate removal by a combination of elemental sulfur-based denitrification and membrane filtration, Water Res. 36 (2002) 1758–1766.
[32] C.M. Oh, C.W. Hwang, T.S. Hwang, Synthesis of a quaternarized poly(vinylimidazole-co-trifluoroethylmethacrylate-co-divinylbenzene) anion-exchange membrane for nitrate removal, J. Environ. Chem. Eng. 2 (2014) 2162–2169.
[33] S.N. Milmile, J.V. Pande, S. Karmakar, A. Bansiwal, T. Chakrabarti, R.B. Biniwale, Equilibrium isotherm and kinetic modeling of the adsorption of nitrates by anion exchange Indion NSSR resin, Desalination 276 (2011) 38–44.
[34] A. Hekmatzadeh, A. Karimi-Jashani, N. Talebbeydokhti, B. Kløve, Modeling of nitrate removal for ion exchange resin in batch and fixed bed experiments, Desalination 284 (2012) 22–31.
[35] H. Song, Y. Zhou, A. Li, S. Mueller, Selective removal of nitrate from water by a macroporous strong basic anion exchange resin, Desalination 296 (2012) 53–60.
[36] M. Alikhani, M. Moghbeli, Ion-exchange polyHIPE type membrane for removing nitrate ions: Preparation, characterization, kinetics and adsorption studies, Chem. Eng. J. 239 (2014) 93–104.
[37] P. Schaetzel, D.N. Amang, Q.T. Nguyen, Batch ion-exchange dialysis to extract nitrate from drinking water: a simplified ion transport model for the best membrane selection, Desalination 164 (2004) 261–268.
[38] N. Barlık, B. Keskinler, M.M. Kocakerim, G. Akay, Surface modification of monolithic polyhipe polymers for anionic functionality and their ion exchange behaviour, J. Appl. Polym. Sci. 132 (2015) 42286–42294.
[39] G. Akay, Flow induced phase inversion in the intensive processing of concentrated emulsions, Chem. Eng. Sci. 53 (1998) 203–223.
[40] G. Akay, Process Intensification and Miniaturization, Encyclopedia of Chemicals Processing, Taylor & Francis, New York, NY, 2006.
[41] S. Brunauer, L.S. Deming, W.E. Deming, E. Teller, On a theory of the van der waals adsorption of gases, J. Am. Chem. Soc. 62 (1940) 1723–1732.
[42] I. Langmuir, The adsorption of gases on plane surfaces of glass, mica and platinum, J. Am. Chem. Soc. 40(9) (1918) 1361–1403.
[43] F. Helfferich, Ion Exchange, McGraw-Hill Inc., New York, NY, 1962.
[44] W. Sherman, The Movement of a Soluble Material During the Washing of a Bed of Packed Solids, Ph. D. Thesis, The Institute of Paper Chemistry, Wisconsin, WI, 1962.
[45] L.D. Benefield, J.F. Judkins, B.L. Weand, Process Chemistry For Water and Wastewater Treatment, Prentice—Hall, Inc., Englewood Cliffs, 1982.